Proceedings of the 9th U.S. National and 10th Canadian Conference on Earthquake Engineering
Compte Rendu de la 9ième Conférence Nationale Américaine et
10ième Conférence Canadienne de Génie Parasismique
July 25-29, 2010, Toronto, Ontario, Canada • Paper No 312

SEISMIC BEHAVIOR OF CIRCULAR CONFINED CONCRETE COLUMNS

S. A. Sheikh[1] and J. Liu[2]

ABSTRACT

This paper reports on seismic behaviour of circular steel-confined concrete columns and the upgrade of deficient columns with fibre reinforced polymers (FRP). Relevant seismic performance data from tests on 15 near full-scale columns is presented. Effectiveness of FRP jackets is evaluated by comparing the behaviour of retrofitted columns with those of similar columns reinforced solely with transverse steel adhering to seismic provisions of various design codes including CSA A23.3-04 and ACI 318-08. Ductility parameters for curvature and displacement are critically examined. An analytical procedure to simulate the behaviour of columns and estimate drift ratio is briefly outlined. A comparison of analytical and experimental column responses shows excellent agreement.

Introduction

It is generally understood that column hinging in concrete structures can not be entirely avoided during severe earthquakes. A comprehensive research program has been underway at the University of Toronto to investigate the seismic performance of square, circular and rectangular reinforced concrete columns (e.g., Sheikh and Uzumeri 1982, Sheikh and Khoury 1993, Sheikh et al. 1994, Sheikh and Khoury 1997, Bayrak and Sheikh 1998). This work has resulted in modeling of fundamental concepts of confinement by lateral steel in rectangular and circular column sections and a procedure for the design of confinement steel in square columns. More recently, this work has concentrated on mitigation of earthquake hazard through strengthening and upgrade of concrete structures with FRP (e.g. Sheikh and Yau 2002, Iacobucci et al 2003, Memon and Sheikh 2005, Ghosh and Sheikh 2007). A design procedure for the upgrade of deficient columns with FRP, developed on the lines of the method for steel-confined columns, has also been recently proposed (Sheikh and Li 2007). A review of the existing work indicated that only limited experimental data exists on circular confined concrete columns especially large scale columns retrofitted with FRP and tested under earthquake loads. This paper thus concentrates on the experimental and analytical behaviour of circular reinforced concrete columns and evaluation of seismic design provisions from different codes. In addition, columns deficient with respect to confining steel are retrofitted with glass or carbon fibre reinforced polymer (GFRP or CFRP) wraps and their responses are evaluated against the steel-confined columns that meet the code provisions.

[1]Professor, Dept. of Civil Engineering, University of Toronto, Toronto, Ontario, Canada
[2]Graduate Research Assistant, Dept. of Civil Engineering, University of Toronto, Toronto, Ontario, Canada

Test Program

Brief details and results from recently completed tests on fifteen columns under simulated earthquake loads are presented here. Each specimen consisted of 356 mm diameter and 1472 mm long column connected with a 508 × 762 × 813 mm stub. Each column had 6-25M (bar area = 500 mm^2) longitudinal bars with a yielding strength of 490 MPa. The lateral reinforcement consisted of #3 (bar area = 71 mm^2) spirals with a yield strength of 496 MPa, except for columns P56-NF-11 and P56-NF-12 (Table 1) in which the spirals were made of 10M (100 mm^2) bars with a yield strength of 450 MPa. The columns were cast together and the compressive cylinder strength of concrete was 40 MPa. All the specimens were subjected to constant axial load and lateral displacement excursions. Fig. 1 shows the schematic of test setup and Fig. 2 shows the idealization of the column specimens. Lateral displacement excursions used for all the tests are shown in Fig. 3. The ductility parameters initially proposed by Sheikh and Khoury (1993) and used to evaluate the behaviour of all columns tested since then, are described in Fig. 4 for a moment-curvature response. The nominal yield curvature ϕ_1 is the curvature at the maximum measured moment M_{max} along a straight line joining the origin and a point of 65% M_{max} on the curve. The ultimate curvature ϕ_2 is the curvature when the post-peak moment capacity reduces to 80% of M_{max}. Similar parameters can also be determined for lateral load-displacement response.

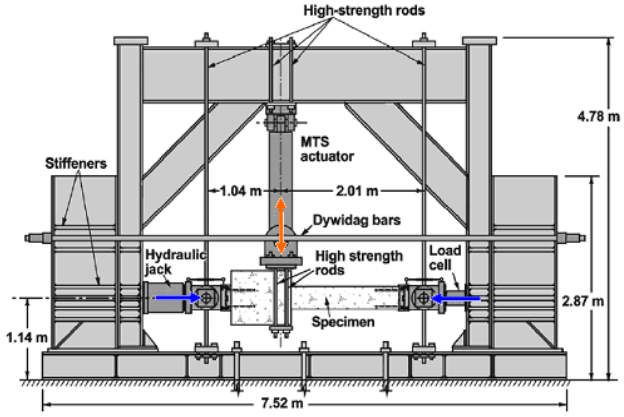

Figure 1. Schematic test setup.

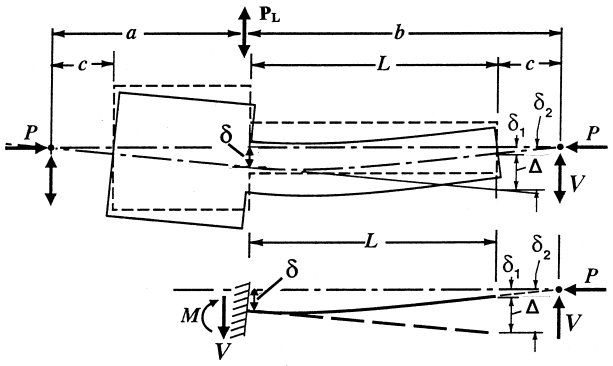

Figure 2. Idealization of column specimens

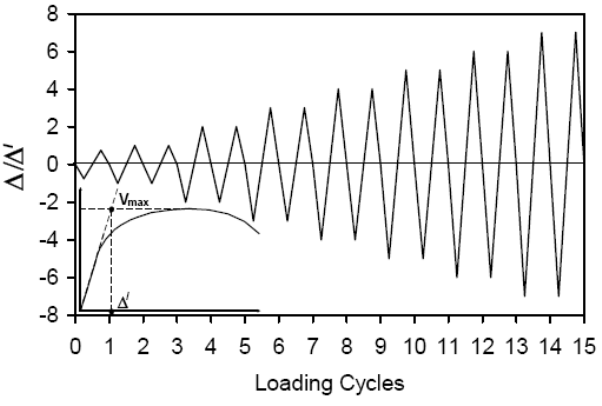

Figure 3. Lateral displacement excursions.

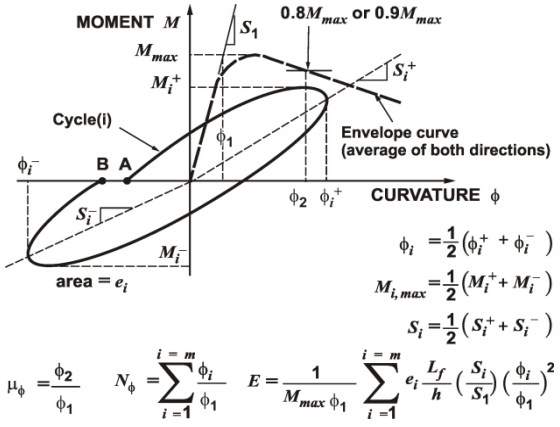

Figure 4. Ductility parameters.

Table 1 shows the details of eight steel-reinforced column specimens while Table 2 provides information about seven column specimens which contained minimal lateral steel reinforcement and were strengthened with lateral FRP wrappings. Tensile strength and stiffness properties of carbon and glass FRP used as external confining reinforcement in retrofitted specimens are also provided in Table 2. Brief results from the tests are shown in the tables. The amount of lateral reinforcement in each column relative to the requirements of various codes is listed in Table 1. In both tables, δ represents lateral drift ratio and is equal to Δ_2/L, where Δ_2 is the deflection corresponding to 20% reduction in lateral load capacity on the descending branch of the shear-deflection (V-Δ) curve and L is the cantilever length of column measured from the section with maximum moment to the point of contraflexure.

Confining Reinforcement Requirements in Various Codes:

The requirements for the volumetric ratio ρ_{sh} of spiral or circular hoop reinforcement in potential plastic hinges from three codes are given below. Eq. 1 gives the requirements of ACI 318-08.

$$\rho_{sh(ACI)} = 0.45\left(\frac{A_g}{A_{ch}} - 1\right)\frac{f_c^{'}}{f_{yh}} \qquad \text{but} \qquad \rho_{sh(ACI)} \geq 0.12\frac{f_c^{'}}{f_{yh}} \tag{1}$$

where A_g = gross area of section; A_{ch} = area of the concrete core measured from the outside of peripheral lateral steel; $f_c^{'}$ = compressive strength of concrete; f_{yh} = yielding strength of lateral steel. These design requirements of $\rho_{sh(ACI)}$ are not targeted at a certain level of ductility performance, and also ignore the influence of applied axial load.

CSA A23.3-04 Code relates the confinement requirements to the applied axial load level and the performance demand measured in terms of curvature ductility factor μ_ϕ. Columns that display curvature ductility factor μ_ϕ equal to or larger than 16 are defined as ductile which is similar to the high ductility columns defined by Sheikh and Khoury (1997). For ductile circular columns, the volumetric ratio $\rho_{sh1(CSA)}$ of spiral or circular hoop reinforcement is given by Eq. 2.

$$\rho_{sh1(CSA)} = 0.40k_p\frac{f_c^{'}}{f_{yh}} \geq 0.45\left(\frac{A_g}{A_{ch}} - 1\right)\frac{f_c^{'}}{f_{yh}} \tag{2}$$

For moderately ductile circular columns (μ_ϕ=10), the required amount of spiral steel $\rho_{sh2(CSA)}$ is provided by Eq. 3. Sheikh and Khoury (1997) had defined moderately ductile columns as having μ_ϕ larger than or equal to 8.

$$\rho_{sh2(CSA)} = 0.30k_p\frac{f_c^{'}}{f_{yh}} \geq 0.45\left(\frac{A_g}{A_{ch}} - 1\right)\frac{f_c^{'}}{f_{yh}} \tag{3}$$

where $k_p = P/P_o$ and all the other terms are defined above.

New Zealand code NZS 3101-1995 requires ductile columns to have a minimum μ_ϕ of 20. For ductile circular columns, the required volumetric ratio $\rho_{sh1(NZS)}$ of spiral reinforcement

according to this code is the larger of the values given by the following two equations:

$$\rho_{sh1(NZS)} = \frac{(1.3 - \rho_t m)}{2.4} \frac{A_g}{A_c} \frac{f_c^{'}}{f_{yt}} \frac{P}{\phi f_c^{'} A_g} - 0.0084 \quad (4)$$

$$\rho_{sh1(NZC)} = \frac{A_{st}}{110 d''} \frac{f_y}{f_{yt}} \frac{1}{d_b} \quad (5)$$

For moderately ductile circular columns which have a minimum μ_ϕ of 10, the larger of the volumes of steel from Equations. 5 and 6 is required.

$$\rho_{sh2(CSA)} = \frac{(1.0 - \rho_t m)}{2.4} \frac{A_g}{A_c} \frac{f_c^{'}}{f_{yt}} \frac{P}{\phi f_c^{'} A_g} - 0.0084 \quad (6)$$

Experimental Results:

As shown in Tables 1 and 2, axial load on four columns was $0.27P_o$, $0.40P_o$ on five columns and six columns were subjected to $0.56P_o$ while they were tested under lateral cyclic displacement excursions. Results listed in the two tables clearly demonstrate the effects of the level of axial load and the amount of lateral reinforcement on column behaviour indicated by curvature and displacement ductility factors and drift ratios. Fig. 5 shows moment-curvature (M-Φ) and shear-deflection (V-Δ) responses of a select group of specimens. As expected (Sheikh and Khoury 1997, Saatcioglu and Baingo 1999, Paultre and Légeron 2008), an increase in axial load results in a significant reduction in column ductility. An increase in the amount of lateral reinforcement enhances column ductility and helps mitigate the adverse effects of axial load on column performance.

The results also show that the displacement ductility factor μ_Δ and drift ratio δ are more consistent parameters to evaluate the column performance than the curvature ductility factor μ_ϕ. For example, measured μ_ϕ for steel-confined columns tested under 0.4 P_o increased from 3.6 to 11.9 with an increase of lateral reinforcement ratio ρ_s from 0.3% to 0.9%, but with further increase of ρ_s to 1.2%, the measured μ_ϕ was still 11.1. The measured μ_Δ and δ, however, showed reasonable trend. The main reason for this discrepancy was observed to be in the difficulty of measuring the largest strains and curvature during the tests. The location of maximum strain at times is not in the instrumented region and thus the measured strains may be substantially underestimated.

The amount of lateral steel provided in the columns varied between 31% and 151% of that required by ACI318-08. The measured column drift ratio δ ranged between 1.3% and 3.7% (Table 1). But it was observed that there was no correlation between the amount of steel required by the code and the deformability of columns. As an example, an amount of steel about 50% larger than that required by the code resulted in approximately 1.9% drift ratio (specimen P56-NF-12) while the amount of lateral steel 40% below the code requirement resulted in drift ratio in excess of 3% (specimen P27-NF-1). This is due to the fact that the axial load level and the ductility performance of columns are not considered as variables in the design of confining reinforcement.

Table 1. Details of steel-confined circular columns

Specimen	Lateral Reinforcement							Axial load level P/P_o	Measured Results				
	Size@spacing (mm)	ρ_s (%)	$\frac{\rho_s}{\rho_{sh(ACI)}}$	$\frac{\rho_s}{\rho_{sh1(CSA)}}$	$\frac{\rho_s}{\rho_{sh2(CSA)}}$	$\frac{\rho_s}{\rho_{sh1(NZS)}}$	$\frac{\rho_s}{\rho_{sh2(NZS)}}$		M_{max} (kNm)	V_{max} (kN)	μ_ϕ	μ_Δ	δ (%)
P27-NF-1	#3@150	0.6	0.61	0.61	0.61	1.51	1.78	0.27	204.2	99.7	11.3	4.3	3.4
P27-NF-2	#3@100	0.9	0.92	0.92	0.92	2.27	2.66	0.27	220.3	100.7	15.6	4.6	3.7
P40-NF-5	#3@300	0.3	0.31	0.23	0.31	0.30	0.79	0.40	180.1	93.0	3.6	3.0	1.7
P40-NF-6	#3@100	0.9	0.92	0.70	0.92	0.91	2.36	0.40	204.8	101.2	11.9	3.5	2.1
P40-NF-7	#3@75	1.2	1.23	0.93	1.23	1.21	3.14	0.40	229.5	107.6	11.1	4.5	2.8
P56-NF-10	#3@300	0.3	0.31	0.17	0.22	0.17	0.34	0.56	188.2	91.1	1.9	2.3	1.3
P56-NF-11	10M@100	1.22	1.13	0.61	0.82	0.61	1.17	0.56	202.9	95.1	10.7	3.4	1.9
P56-NF-12	10M@75	1.63	1.51	0.82	1.09	0.82	1.56	0.56	197.3	93.0	13.2	3.2	1.9

Table 2. Details of FRP-confined circular columns

Specimen	Lateral Reinforcement					Axial load level P/P_o	Measured Results				
	Size@spacing (mm)	ρ_s (%)	FRP retrofit	f_{uFRP} (MPa)	E_{FRP} (MPa)		M_{max} (kNm)	V_{max} (kN)	μ_ϕ	μ_Δ	δ (%)
P27-1CF-3	#3@300	0.3	1-Layer 1.00mm CFRP	939	76433	0.27	264.3	118.6	12.9	4.3	4.2
P27-2GF-4	#3@300	0.3	2-Layer 1.25mm GFRP	518	25488	0.27	250.7	105.2	10.6	4.4	4.6
P40-1CF-8	#3@300	0.3	1-Layer 1.00mm CFRP	939	76433	0.40	261.2	98.7	9.2	4.6	4.0
P40-1GF-9	#3@300	0.3	1-Layer 1.25mm GFRP	518	25488	0.40	257.5	115.5	8.2	4.3	3.1
P40-2CF-13	#3@300	0.3	2-Layer 1.00mm CFRP	939	76433	0.40	331.1	97.7	6.8	5.3	4.0
P56-3GF-14	#3@300	0.3	3-Layer 1.25mm GFRP	518	25488	0.56	337.4	109.6	8.4	5.2	3.5
P56-4GF-15	#3@300	0.3	4-Layer 1.25mm GFRP	518	25488	0.56	363.9	118.6	11.1	5.0	3.6

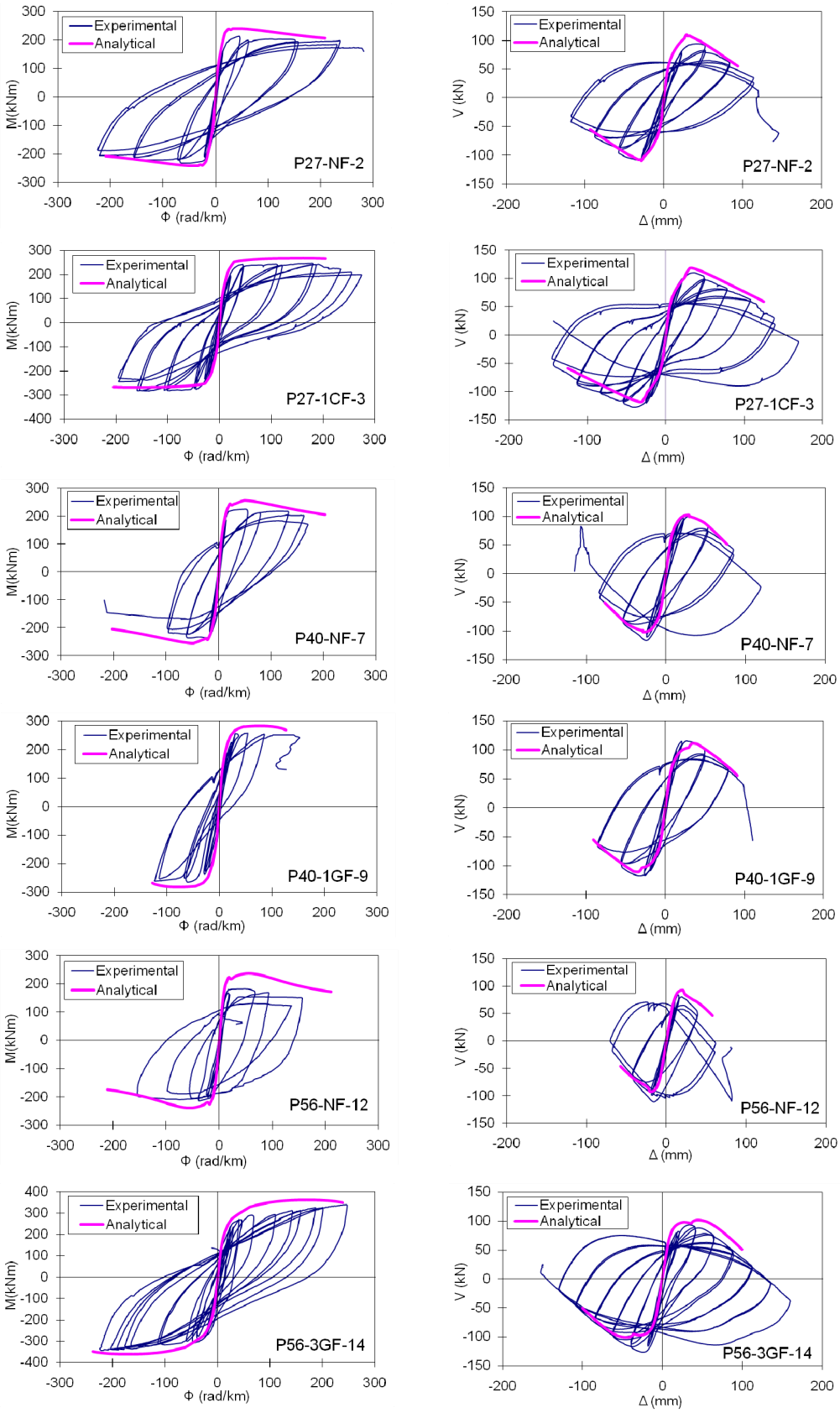

Figure 5. Moment-curvature and shear-deflection responses of columns

For the Canadian code (CSA A23.3-04) and New Zealand code (NZS 3101-1995), two values for ρ_s/ρ_{sh} are shown in Table 1 since different equations govern the design of lateral reinforcement depending on the level of curvature ductility required. Considering the experimental curvature ductility ratios, none of the steel-confined columns can be classified as ductile except P27-NF-2 which has a μ_ϕ of 15.6 and can perhaps be defined as ductile according to the Canadian code. For columns which have μ_ϕ of about 10, $\rho_s/\rho_{sh2\ (CSA)}$ varied between 0.61 and 1.23. For columns with μ_ϕ of about 13, $\rho_s/\rho_{sh2\ (CSA)}$ varied between 0.92 and 1.09. The corresponding values for the New Zealand code (NZS 3101-1995) are considerably larger indicating that this code requires much less confining steel compared with the Canadian code.

It is noted that the relationships between the amount of lateral confinement and the different ductility factors (μ_ϕ, μ_Δ or δ) vary significantly under different levels of axial load. The curvature ductility factor μ_ϕ increased with an increase in lateral reinforcement for almost all the specimens. However, the displacement ductility factor μ_Δ and drift ratio δ do not change significantly when columns are subjected to very high axial load level ($0.56P/P_o$). Compared with P56-NF-11, column P56-NF-12 contained about 30% more confinement and displayed equally higher μ_ϕ value, but μ_Δ and δ were almost equal in both columns. Similar observations can also be made for columns P56-2CF-13, P56-3GF-14 and P56-4GF-15. This is due to the fact that most of the moment capacity at the critical section in columns under high axial loads is consumed by the P-Δ effect. An increase in the confinement reinforcement thus may not achieve higher displacement ductility despite providing higher curvature ductility.

Analytical Results:

An iterative incremental procedure, to determine the behaviour of concrete confined with FRP, was developed by Cui and Sheikh (2009) based on compressive behavior of concrete, tensile properties of FRP and interaction between concrete and FRP. Four quadrants of relationships are required for the modeling (Fig. 6): Quadrant I contains the axial stress-strain relationships of concrete, each under a different constant confining stress; Quadrant II is for the relationship between the axial strain and the lateral strain of concrete under constant confinement; Quadrant III displays the stress-strain relationship of FRP; and Quadrant IV is the relationship between confining stress in concrete and the tension stress in FRP. As illustrated in the figure, the loading is applied by imposing an axial strain ε_c^i. Starting from an assumed lateral confining stress f_{con}^*, the lateral strain ε_l can be obtained from the dilation properties of concrete (Quadrant II). The lateral strain is then used to determine the stress in the FRP jacket based on the properties of FRP (Quadrant III). After that, the confining pressure exerted by FRP jackets $f_{con}^\#$ can be calculated (Quadrant IV). This calculated lateral confining pressure is compared with the assumed initial value of f_{con}^*. If they are inconsistent, the average of these confining pressures will be applied to start the next iteration of above calculations. This will be repeated until the lateral confining stress is converged at f_{con}^i. Finally, f_{con}^i is applied to find the appropriate axial stress-strain curve of confined concrete in Quadrant I. From this curve, we can find the confined concrete stress for the imposed axial strain ε_c^i. This represents one point on the required stress-strain plot of the FRP-confined concrete. The complete stress-strain response can be obtained by finding stresses for different axial strains using this procedure.

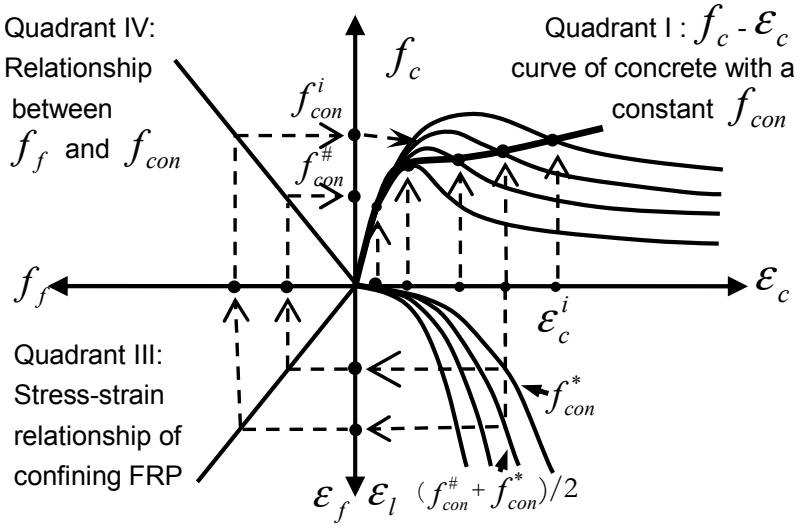

Figure 6. Constitutive model for confined concrete (Cui and Sheikh 2009)

For steel-confined concrete, the above iterative procedure is not necessary. The lateral confining stress is basically deemed as constant with the expansion of concrete after the yielding of confining steel. Therefore, the axial stress-strain relationships in quadrant I can be directly used corresponding to different level of confining stress.

A computation program that uses the stress-strain model described above for confined concrete was developed to conduct push-over analysis of cantilever columns. It is applicable to square or circular columns, which are laterally confined by steel or FRP jackets. The concrete strength ranges from 25 MPa to 110 MPa. The program consists of two parts: sectional analysis to obtain moment-curvature (M- Φ) response, and elemental analysis to determine the shear-deflection (V-Δ) behaviour. Fig. 5 also presents the analytical curves obtained using this procedure along with the experimental results. Analytical M- Φ and V-Δ curves represent the envelop curves of measured hysteresis loops quite well. Generally the predictions for V-Δ curves are much better than those for M- Φ. As discussed above, this appears to be due to the inherent difficulties in measuring the strain values during the tests that are used to calculate the curvature vales.

Summary and Conclusions

Results from a test series consisting of 15 circular columns tested under simulated earthquake loads are presented. Each specimen consisted of 356 mm diameter and 1472 mm long column connected with a 508 × 762 × 813 mm stub. Each column had 6-25M (bar area = 500 mm^2) longitudinal bars. Different amounts of lateral spiral steel were used in eight columns to evaluate the requirements of various design codes. Seven columns containing minimum amount of lateral steel were retrofitted with glass or carbon FRP wrapping to enhance their seismic resistance. The main variables that affect the ductility and energy dissipation capacity of a column include the level of axial load and the type and amount of confining reinforcement. An increase in the level of axial load and ductility demand significantly raises the requirements of

lateral confinement in a column. The confinement requirements of ACI318-08 were found to be totally disconnected from the performance levels of columns. The Canadian and New Zealand Codes provide the design of confining reinforcement for a target curvature ductility level but the amount of steel required varied greatly between the two codes with NZS code requiring much smaller amount of lateral steel in most cases.

An analytical procedure has been developed to conduct push-over analysis of cantilever columns to obtain moment-curvature (M- Φ) response and the shear-deflection (V-Δ) behaviour. It is applicable to square or circular columns, which are laterally confined by steel or FRP jackets. Results presented here show that the analytical M- Φ and V-Δ responses simulate the envelop curves of measured hysteresis loops quite well.

References

ACI Committee 318, 2008. *Building Code Requirements for Structural Concrete* (ACI 318-08). Farmington Hills (MI): American Concrete Institute.

Bayrak, O., and Sheikh, S. A., 1998. Confinement reinforcement design considerations for ductile HSC columns, *Journal of Structural Engineering,* ASCE, 124(9), 999-1010.

CSA-A23.3-04, 2004. *Design of Concrete Structures*. Canadian Standards Association, Rexdale, Ontario, Canada.

Cui, C., and Sheikh, S. A., 2009. Analytical model for normal- and high- strength concrete confined with fiber reinforced polymers, *Journal of Structural Engineering,* ASCE, (submitted for publication).

Ghosh, K. K., and Sheikh, S. A., 2007. Seismic upgrade with carbon fiber-reinforced polymer of columns containing lap-spliced reinforcing bars, *ACI Structural Journal*, 104(2), 227-236.

Iacobucci, R. D.; Sheikh, S. A.; and Bayrak, O., 2003. Retrofit of square concrete columns with carbon fiber-reinforced polymer for seismic resistance, *ACI Structural Journal*, 100(6), 785-794.

Liu, J., and Sheikh, S. A., 2009. Seismic behavior of steel-confined and FRP-confined circular concrete columns, *Research Report*, Department of Civil Engineering, University of Toronto, Canada.

Memon, M. S., and Sheikh, S. A., 2005, Seismic resistance of square concrete columns retrofitted with glass fiber-reinforced polymer, *ACI Structural Journal*, 102(5), 774-783.

NZS-3101, 1995. *New Zealand Standard Code of Practice for the Design of Concrete Structures*, Standards Association of New Zealand, Wellington, New Zealand.

Paultre, P., and Légeron, F., 2008. Confinement reinforcement design for reinforced concrete columns, Journal of Structiural Engineering, *ASCE*, 134(5), 738-749.

Saatcioglu, M., and Baingo, D., 1999. Circular high-strength concrete columns under simulated seismic loading, *Journal of Structural Engineering*, *ASCE,* 125(3), 272–280.

Sheikh, S. A., and Khoury S. S., 1993. Confined concrete columns with stubs, *ACI Structural Journal*, 90(4), 414-431.

Sheikh, S. A., Khoury, S. S., 1997. A performance-based approach for the design of confining steel in tied columns, *ACI Structural Journal*, 94(4), 421-431.

Sheikh, S. A., and Li, Y., 2007. "Design of FRP confinement for Square Concrete Columns", *Journal of Engineering Structures,* 29(6), 1074-1083.

Sheikh, S.A.; Shah, D.V.; and Khoury, S.S., 1994. Confinement of high-strength concrete columns, *ACI Structural Journal*, 91(1), 100-111.

Sheikh, S.A., and Uzumeri, S.M., 1982. Analytical model for concrete confinement in tied columns, *Journal of the Structural Division, ASCE,* 109(ST12), 2703-2722.

Sheikh, S. A., and Yau, G., 2002. Seismic behavior of concrete columns confined with steel and fiber-reinforced polymers," *ACI Structural Journal*, 99(1), 72-80.